INSTITUTE OF PHYSICS PUBLISHING JOURNAL OF PHYSICS A: MATHEMATICAL AND GENERAL

J. Phys. A: Math. Gen. **38** (2005) 5531–5546 doi:10.1088/0305-4470/38/24/007

Unfolding of eigenvalue surfaces near a diabolic point due to a complex perturbation

O N Kirillov, A A Mailybaev and A P Seyranian

Institute of Mechanics, Moscow State Lomonosov University, Michurinskii pr. 1, 119192 Moscow, Russia

E-mail: kirillov@imec.msu.ru, mailybaev@imec.msu.ru and seyran@imec.msu.ru

Received 1 November 2004, in final form 8 April 2005
Published 1 June 2005
Online at stacks.iop.org/JPhysA/38/5531

Abstract

The paper presents a new theory of unfolding of eigenvalue surfaces of real symmetric and Hermitian matrices due to an arbitrary complex perturbation near a diabolic point. General asymptotic formulae describing deformations of a conical surface for different kinds of perturbing matrices are derived. As a physical application, singularities of the surfaces of refractive indices in crystal optics are studied.

PACS numbers: 03.65.Vf, 32.60.+i

1. Introduction

Since the papers by Von Neumann and Wigner (1929) and Teller (1937), it is known that the energy surfaces in quantum physics may cross forming two sheets of a double cone: a diabolo. The apex of the cone is called a diabolic point, see Berry and Wilkinson (1984). This kind of crossing is typical for systems described by real symmetric Hamiltonians with at least two parameters and Hermitian Hamiltonians depending on three or more parameters. From a mathematical point of view, the energy surfaces are described by eigenvalues of real symmetric or Hermitian operators dependent on parameters, and the diabolic point is a point of a double eigenvalue with two linearly independent eigenvectors. In modern problems of quantum physics, crystal optics, physical chemistry, acoustics and mechanics, it is important to know how the diabolic point bifurcates under arbitrary complex perturbations forming topological singularities of eigenvalue surfaces like a double coffee filter with two exceptional points or a diabolic circle of exceptional points, see e.g. Mondragon and Hernandez (1993, 1996), Shuvalov and Scott (2000), Keck *et al* (2003), Berry and Dennis (2003), Korsch and Mossmann (2003) and Berry (2004).

In our preceding companion paper (Seyranian *et al* 2005), a general theory of coupling of eigenvalues for complex matrices of arbitrary dimension smoothly depending on multiple real parameters was presented. Two kinds of important singularities were mathematically

classified: the diabolic points (DPs) and the exceptional points (EPs). DP is a point where the eigenvalues coalesce, while corresponding eigenvectors remain different (linearly independent), and EP is a point where both eigenvalues and eigenvectors coalesce forming a Jordan block. General formulae describing coupling and decoupling of eigenvalues, crossing and avoided crossing of eigenvalue surfaces were derived. Both the DP and EP cases are interesting in applications and were observed in experiments, see Ramachandran and Ramaseshan (1961), Dembowsky *et al* (2001, 2003) and Stehmann *et al* (2004).

In the present paper following the theory developed in Seyranian *et al* (2005) we study effects of complex perturbations in multiparameter families of real symmetric and Hermitian matrices. In the case of real symmetric matrices we study the unfolding of eigenvalue surfaces near a diabolic point under real and complex perturbations. The origination of singularities such as a 'double coffee filter' and a 'diabolic circle' is analytically described. Unfolding of a diabolic point of a Hermitian matrix under an arbitrary complex perturbation is analytically treated. We emphasize that the unfolding of eigenvalue surfaces is described qualitatively as well as quantitatively by using only the information at the diabolic point, including eigenvalues, eigenvectors and derivatives of the system matrix taken at the diabolic point.

As a physical application, singularities of the surfaces of refractive indices in crystal optics are studied. Asymptotic formulae for the metamorphoses of these surfaces depending on properties of a crystal are established and discussed in detail. Singular axes for general crystals with weak absorption and chirality are found. A new explicit condition distinguishing the absorption-dominated and chirality-dominated crystals is established in terms of components of the inverse dielectric tensor. Numerical examples are given to illustrate the general theory.

2. Asymptotic expressions for eigenvalues near a diabolic point

Let us consider the eigenvalue problem

$$\mathbf{A}\mathbf{u} = \lambda\mathbf{u} \tag{1}$$

for an $m \times m$ Hermitian matrix $\mathbf{A}$, where λ is an eigenvalue and $\mathbf{u}$ is an eigenvector. Such eigenvalue problems arise in non-dissipative physics with and without time reversal symmetry. Real symmetric and complex Hermitian matrices correspond to these two cases, respectively. We assume that the matrix $\mathbf{A}$ smoothly depends on a vector of n real parameters $\mathbf{p} = (p_1, \ldots, p_n)$. Let λ_0 be a double eigenvalue of the matrix $\mathbf{A}_0 = \mathbf{A}(\mathbf{p}_0)$ for some vector $\mathbf{p}_0$. Since $\mathbf{A}_0$ is a Hermitian matrix, the eigenvalue λ_0 is real and possesses two eigenvectors $\mathbf{u}_1$ and $\mathbf{u}_2$. Thus, the point of eigenvalue coupling for Hermitian matrices is diabolic. We choose the eigenvectors satisfying the normalization conditions

$$(\mathbf{u}_1, \mathbf{u}_1) = (\mathbf{u}_2, \mathbf{u}_2) = 1, \qquad (\mathbf{u}_1, \mathbf{u}_2) = 0, \tag{2}$$

where the standard inner product of complex vectors is given by $(\mathbf{u}, \mathbf{v}) = \sum_{i=1}^{m} u_i \overline{v}_i$.

Under perturbation of parameters $\mathbf{p} = \mathbf{p}_0 + \Delta\mathbf{p}$, the bifurcation of λ_0 into two simple eigenvalues λ_+ and λ_- occurs. The asymptotic formula for $\lambda_\pm$ under multiparameter perturbation is (Seyranian *et al* 2005)

$$\lambda_\pm = \lambda_0 + \frac{\langle \mathbf{f}_{11} + \mathbf{f}_{22}, \Delta\mathbf{p}\rangle}{2} \pm \sqrt{\frac{\langle \mathbf{f}_{11} - \mathbf{f}_{22}, \Delta\mathbf{p}\rangle^2}{4} + \langle \mathbf{f}_{12}, \Delta\mathbf{p}\rangle\langle \mathbf{f}_{21}, \Delta\mathbf{p}\rangle}. \tag{3}$$

Components of the vector $\mathbf{f}_{ij} = \left(f_{ij}^1, \ldots, f_{ij}^n\right)$ are

$$f_{ij}^k = \left(\frac{\partial \mathbf{A}}{\partial p_k}\mathbf{u}_i, \mathbf{u}_j\right), \tag{4}$$

where the derivative is taken at $\mathbf{p}_0$, and inner products of vectors in (3) are given by $\langle \mathbf{a}, \mathbf{b} \rangle = \sum_{i=1}^{n} a_i \overline{b}_i$. Note that we use different notation for the inner product to distinguish between the linear complex space C^m (round brackets) and linear real space R^n (angular brackets). In expression (3), the higher-order terms $o(\|\Delta\mathbf{p}\|)$ and $o(\|\Delta\mathbf{p}\|^2)$ are omitted before and under the square root. Since the matrix $\mathbf{A}$ is Hermitian, the vectors $\mathbf{f}_{11}$ and $\mathbf{f}_{22}$ are real and the vectors $\mathbf{f}_{12} = \overline{\mathbf{f}}_{21}$ are complex conjugate. In the case of real symmetric matrices $\mathbf{A} = \mathbf{A}^T$, the vectors $\mathbf{f}_{11}, \mathbf{f}_{22}$ and $\mathbf{f}_{12} = \mathbf{f}_{21}$ are real. The asymptotic expression for the eigenvectors corresponding to $\lambda_\pm$ takes the form (Seyranian *et al* 2005)

$$\mathbf{u}_\pm = \alpha_\pm \mathbf{u}_1 + \beta_\pm \mathbf{u}_2, \qquad \frac{\alpha_\pm}{\beta_\pm} = \frac{\langle \mathbf{f}_{12}, \Delta\mathbf{p} \rangle}{\lambda_\pm - \lambda_0 - \langle \mathbf{f}_{11}, \Delta\mathbf{p} \rangle} = \frac{\lambda_\pm - \lambda_0 - \langle \mathbf{f}_{22}, \Delta\mathbf{p} \rangle}{\langle \mathbf{f}_{21}, \Delta\mathbf{p} \rangle}. \tag{5}$$

Expressions (5) provide zero-order terms for the eigenvectors $\mathbf{u}_\pm$ under perturbation of the parameter vector.

Now, consider an arbitrary complex perturbation of the matrix family $\mathbf{A}(\mathbf{p}) + \Delta\mathbf{A}(\mathbf{p})$. Such perturbations appear due to non-conservative effects breaking symmetry of the initial system. We assume that the size of perturbation $\Delta\mathbf{A}(\mathbf{p}) \sim \varepsilon$ is small, where $\varepsilon = \|\Delta\mathbf{A}(\mathbf{p}_0)\|$ is the Frobenius norm of the perturbation at the diabolic point. Behaviour of the eigenvalues $\lambda_\pm$ for small $\Delta\mathbf{p}$ and small ε is described by the following asymptotic formula (Seyranian *et al* 2005):

$$\lambda_\pm = \lambda_0 + \frac{\langle \mathbf{f}_{11} + \mathbf{f}_{22}, \Delta\mathbf{p} \rangle}{2} + \frac{\varepsilon_{11} + \varepsilon_{22}}{2} \pm \sqrt{\frac{(\langle \mathbf{f}_{11} - \mathbf{f}_{22}, \Delta\mathbf{p} \rangle + \varepsilon_{11} - \varepsilon_{22})^2}{4} + (\langle \mathbf{f}_{12}, \Delta\mathbf{p} \rangle + \varepsilon_{12})(\langle \mathbf{f}_{21}, \Delta\mathbf{p} \rangle + \varepsilon_{21})}. \tag{6}$$

The quantities ε_{ij} are small complex numbers of order ε given by the expression

$$\varepsilon_{ij} = (\Delta\mathbf{A}(\mathbf{p}_0)\mathbf{u}_i, \mathbf{u}_j). \tag{7}$$

A small variation of the matrix family leads to the following correction of the asymptotic expression for the eigenvectors:

$$\mathbf{u}_\pm = \alpha^\varepsilon_\pm \mathbf{u}_1 + \beta^\varepsilon_\pm \mathbf{u}_2, \qquad \frac{\alpha^\varepsilon_\pm}{\beta^\varepsilon_\pm} = \frac{\langle \mathbf{f}_{12}, \Delta\mathbf{p} \rangle + \varepsilon_{12}}{\lambda_\pm - \lambda_0 - \langle \mathbf{f}_{11}, \Delta\mathbf{p} \rangle - \varepsilon_{11}} = \frac{\lambda_\pm - \lambda_0 - \langle \mathbf{f}_{22}, \Delta\mathbf{p} \rangle - \varepsilon_{22}}{\langle \mathbf{f}_{21}, \Delta\mathbf{p} \rangle + \varepsilon_{21}}. \tag{8}$$

The ratios $\alpha^\varepsilon_+ / \beta^\varepsilon_+ = \alpha^\varepsilon_- / \beta^\varepsilon_-$ at the point of coincident eigenvalues $\lambda_+ = \lambda_-$. Hence, the eigenvectors $\mathbf{u}_+ = \mathbf{u}_-$ coincide, and the point of eigenvalue coupling of the perturbed system becomes exceptional (EP). For some specific perturbations $\Delta\mathbf{A}(\mathbf{p})$, the coupling point may remain diabolic under the conditions

$$\langle \mathbf{f}_{12}, \Delta\mathbf{p} \rangle + \varepsilon_{12} = 0, \qquad \langle \mathbf{f}_{21}, \Delta\mathbf{p} \rangle + \varepsilon_{21} = 0, \qquad \langle \mathbf{f}_{11} - \mathbf{f}_{22}, \Delta\mathbf{p} \rangle + \varepsilon_{11} - \varepsilon_{22} = 0, \tag{9}$$

when both ratios in (8) become undetermined.

We observe that an asymptotic description of unfolding of a diabolic singularity due to perturbation of the matrix family requires only the value of $\Delta\mathbf{A}(\mathbf{p})$ taken at the coupling point $\mathbf{p}_0$. Dependence of the perturbation $\Delta\mathbf{A}$ on the vector of parameters $\mathbf{p}$ near the point $\mathbf{p}_0$ is not so important, since it influences higher-order terms.

3. Unfolding of a diabolic singularity for real symmetric matrices

Let us assume that $\mathbf{A}(\mathbf{p})$ is an n-parameter family of real symmetric matrices. Then its eigenvalues λ are real. Let λ_0 be a double eigenvalue of the matrix $\mathbf{A}_0 = \mathbf{A}(\mathbf{p}_0)$ with two real

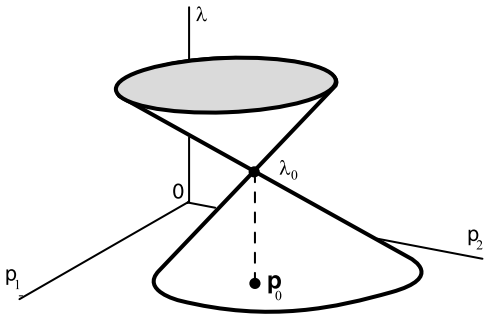

Figure 1. A diabolic point in a family of real symmetric matrices.

eigenvectors $\mathbf{u}_1$ and $\mathbf{u}_2$. Under perturbation of parameters $\mathbf{p} = \mathbf{p}_0 + \Delta\mathbf{p}$, the eigenvalue λ_0 splits into two simple eigenvalues λ_+ and λ_-. The asymptotic formula for $\lambda_\pm$ under multiparameter perturbation is given by equations (3) and (4), where the vectors $\mathbf{f}_{11}$, $\mathbf{f}_{22}$ and $\mathbf{f}_{12} = \mathbf{f}_{21}$ are real. Then, equation (3) takes the form

$$\left(\lambda_\pm - \lambda_0 - \frac{\langle \mathbf{f}_{11} + \mathbf{f}_{22}, \Delta\mathbf{p}\rangle}{2}\right)^2 - \frac{\langle \mathbf{f}_{11} - \mathbf{f}_{22}, \Delta\mathbf{p}\rangle^2}{4} - \langle \mathbf{f}_{12}, \Delta\mathbf{p}\rangle^2 = 0. \tag{10}$$

Equation (10) describes a surface in the space $(p_1, p_2, \ldots, p_n, \lambda)$, which consists of two sheets $\lambda_+(\mathbf{p})$ and $\lambda_-(\mathbf{p})$. These sheets are connected at the points satisfying the equations

$$\lambda_\pm = \lambda_0 + \tfrac{1}{2}\langle \mathbf{f}_{11} + \mathbf{f}_{22}, \Delta\mathbf{p}\rangle, \qquad \langle \mathbf{f}_{11} - \mathbf{f}_{22}, \Delta\mathbf{p}\rangle = 0, \qquad \langle \mathbf{f}_{12}, \Delta\mathbf{p}\rangle = 0, \tag{11}$$

where the eigenvalues couple: $\lambda_+ = \lambda_-$. Equations (11) define a plane of dimension $n - 2$. Thus, the double eigenvalue is a phenomenon of codimension 2 in an n-parameter family of real symmetric matrices (Von Neumann and Wigner 1929).

For the two-parameter matrix $\mathbf{A}(p_1, p_2)$, equation (10) defines a double cone with apex at the point $(\mathbf{p}_0, \lambda_0)$ in the space (p_1, p_2, λ), see figure 1. The point $(\mathbf{p}_0, \lambda_0)$ is referred to as a 'diabolic point' (Berry and Wilkinson 1984) due to the conical shape of the children's toy 'diabolo'.

Let us consider a perturbation $\mathbf{A}(\mathbf{p}) + \Delta\mathbf{A}(\mathbf{p})$ of the real symmetric family $\mathbf{A}(\mathbf{p})$ in the vicinity of the diabolic point $\mathbf{p}_0$, where $\Delta\mathbf{A}(\mathbf{p})$ is a complex matrix with the small norm $\varepsilon = \|\Delta\mathbf{A}(\mathbf{p}_0)\|$. Splitting of the double eigenvalue λ_0 due to a change of the vector of parameters $\Delta\mathbf{p}$ and a small complex perturbation $\Delta\mathbf{A}$ is described by equation (6), which acquires the form

$$\lambda_\pm = \lambda_0' + \mu \pm \sqrt{c}, \qquad c = (x + \xi)^2 + (y + \eta)^2 - \zeta^2. \tag{12}$$

In equation (12), the quantities λ_0', x and y are real,

$$\lambda_0' = \lambda_0 + \tfrac{1}{2}\langle \mathbf{f}_{11} + \mathbf{f}_{22}, \Delta\mathbf{p}\rangle, \qquad x = \tfrac{1}{2}\langle \mathbf{f}_{11} - \mathbf{f}_{22}, \Delta\mathbf{p}\rangle, \qquad y = \langle \mathbf{f}_{12}, \Delta\mathbf{p}\rangle, \tag{13}$$

while the small coefficients μ, ξ, η and ζ are complex:

$$\mu = \tfrac{1}{2}(\varepsilon_{11} + \varepsilon_{22}), \qquad \xi = \tfrac{1}{2}(\varepsilon_{11} - \varepsilon_{22}), \qquad \eta = \tfrac{1}{2}(\varepsilon_{12} + \varepsilon_{21}), \qquad \zeta = \tfrac{1}{2}(\varepsilon_{12} - \varepsilon_{21}). \tag{14}$$

Separating real and imaginary parts in equation (12), we find

$$\begin{aligned} &\mathrm{Re}^2(\lambda - \lambda_0' - \mu) - \mathrm{Im}^2(\lambda - \lambda_0' - \mu) = \mathrm{Re}\, c, \\ &2\,\mathrm{Re}(\lambda - \lambda_0' - \mu)\mathrm{Im}(\lambda - \lambda_0' - \mu) = \mathrm{Im}\, c, \end{aligned} \tag{15}$$

where

$$\operatorname{Re} c = (\operatorname{Im}^2 \zeta - \operatorname{Im}^2 \xi - \operatorname{Im}^2 \eta - \operatorname{Re}^2 \zeta) + (x + \operatorname{Re} \xi)^2 + (y + \operatorname{Re} \eta)^2, \tag{16}$$

$$\operatorname{Im} c = 2((x + \operatorname{Re} \xi)\operatorname{Im} \xi + (y + \operatorname{Re} \eta)\operatorname{Im} \eta - \operatorname{Re} \zeta \operatorname{Im} \zeta). \tag{17}$$

From equations (15), we get the expressions determining the real and imaginary parts of the perturbed eigenvalues,

$$\operatorname{Re} \lambda_\pm = \lambda_0' + \operatorname{Re} \mu \pm \sqrt{(\operatorname{Re} c + \sqrt{\operatorname{Re}^2 c + \operatorname{Im}^2 c})/2}, \tag{18}$$

$$\operatorname{Im} \lambda_\pm = \operatorname{Im} \mu \pm \sqrt{(-\operatorname{Re} c + \sqrt{\operatorname{Re}^2 c + \operatorname{Im}^2 c})/2}. \tag{19}$$

Strictly speaking, for the same eigenvalue one should take equal or opposite signs before the square roots in (18), (19) for positive or negative $\operatorname{Im} c$, respectively.

Equations (18) and (19) define surfaces in the spaces $(p_1, p_2, \ldots, p_n, \operatorname{Re} \lambda)$ and $(p_1, p_2, \ldots, p_n, \operatorname{Im} \lambda)$. Two sheets of the surface (18) are connected ($\operatorname{Re} \lambda_+ = \operatorname{Re} \lambda_-$) at the points satisfying the conditions

$$\operatorname{Re} c \leqslant 0, \qquad \operatorname{Im} c = 0, \qquad \operatorname{Re} \lambda_\pm = \lambda_0' + \operatorname{Re} \mu, \tag{20}$$

while the sheets $\operatorname{Im} \lambda_+(\mathbf{p})$ and $\operatorname{Im} \lambda_-(\mathbf{p})$ are glued at the set of points satisfying

$$\operatorname{Re} c \geqslant 0, \qquad \operatorname{Im} c = 0, \qquad \operatorname{Im} \lambda_\pm = \operatorname{Im} \mu. \tag{21}$$

Note that in the neighbourhood of the intersections (20) and (21) the eigenvalue sheets given by formulae (18) and (19) can be described by the following approximate expressions:

$$\begin{aligned} &\operatorname{Re} \lambda_\pm = \lambda_0' + \operatorname{Re} \mu \pm \frac{\operatorname{Im} c}{2} \sqrt{\frac{-1}{\operatorname{Re} c}}, && \operatorname{Re} c < 0; \\ &\operatorname{Im} \lambda_\pm = \operatorname{Im} \mu \pm \frac{\operatorname{Im} c}{2} \sqrt{\frac{1}{\operatorname{Re} c}}, && \operatorname{Re} c > 0. \end{aligned} \tag{22}$$

The eigenvalue remains double under the perturbation of parameters when $c = 0$, which yields two equations $\operatorname{Re} c = 0$ and $\operatorname{Im} c = 0$. Two cases are distinguished according to the sign of the quantity

$$D = \operatorname{Im}^2 \xi + \operatorname{Im}^2 \eta - \operatorname{Im}^2 \zeta. \tag{23}$$

If $D > 0$, then the equations $\operatorname{Re} c = 0$ and $\operatorname{Im} c = 0$, with expressions (16), (17), yield two solutions (x_a, y_a) and (x_b, y_b), where

$$x_{a,b} = \frac{\operatorname{Im} \xi \operatorname{Re} \zeta \operatorname{Im} \zeta \pm \operatorname{Im} \eta \sqrt{(\operatorname{Im}^2 \xi + \operatorname{Im}^2 \eta + \operatorname{Re}^2 \zeta)(\operatorname{Im}^2 \xi + \operatorname{Im}^2 \eta - \operatorname{Im}^2 \zeta)}}{\operatorname{Im}^2 \xi + \operatorname{Im}^2 \eta} - \operatorname{Re} \xi, \tag{24}$$

$$y_{a,b} = \frac{\operatorname{Im} \eta \operatorname{Re} \zeta \operatorname{Im} \zeta \mp \operatorname{Im} \xi \sqrt{(\operatorname{Im}^2 \xi + \operatorname{Im}^2 \eta + \operatorname{Re}^2 \zeta)(\operatorname{Im}^2 \xi + \operatorname{Im}^2 \eta - \operatorname{Im}^2 \zeta)}}{\operatorname{Im}^2 \xi + \operatorname{Im}^2 \eta} - \operatorname{Re} \eta. \tag{25}$$

These two solutions determine the points in parameter space, where double eigenvalues appear. When $D = 0$, the two solutions coincide. For $D < 0$, the equations $\operatorname{Re} c = 0$ and $\operatorname{Im} c = 0$ have no real solutions. In the latter case, the eigenvalues λ_+ and λ_- separate for all $\Delta\mathbf{p}$.

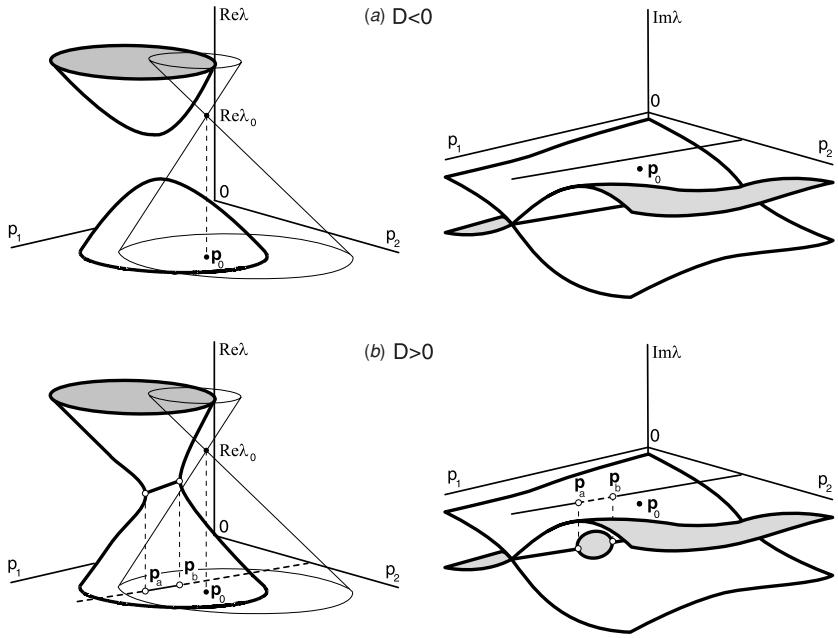

Figure 2. Unfolding of a diabolic point due to complex perturbation.

Note that the quantities $\operatorname{Im}\xi$ and $\operatorname{Im}\eta$ are expressed by means of the anti-Hermitian part $\Delta\mathbf{A}_N = (\Delta\mathbf{A} - \overline{\Delta\mathbf{A}}^T)/2$ of the matrix $\Delta\mathbf{A}$ as

$$\operatorname{Im}\xi = \frac{(\Delta\mathbf{A}_N(\mathbf{p}_0)\mathbf{u}_1, \mathbf{u}_1) - (\Delta\mathbf{A}_N(\mathbf{p}_0)\mathbf{u}_2, \mathbf{u}_2)}{2\mathrm{i}},$$
$$\operatorname{Im}\eta = \frac{(\Delta\mathbf{A}_N(\mathbf{p}_0)\mathbf{u}_1, \mathbf{u}_2) + (\Delta\mathbf{A}_N(\mathbf{p}_0)\mathbf{u}_2, \mathbf{u}_1)}{2\mathrm{i}}, \tag{26}$$

while $\operatorname{Im}\zeta$ depends on the Hermitian part $\Delta\mathbf{A}_H = (\Delta\mathbf{A} + \overline{\Delta\mathbf{A}}^T)/2$ as

$$\operatorname{Im}\zeta = \frac{(\Delta\mathbf{A}_H(\mathbf{p}_0)\mathbf{u}_1, \mathbf{u}_2) - (\Delta\mathbf{A}_H(\mathbf{p}_0)\mathbf{u}_2, \mathbf{u}_1)}{2\mathrm{i}}. \tag{27}$$

If $D > 0$, one can say that the influence of the anti-Hermitian part of the perturbation $\Delta\mathbf{A}$ is stronger than that of the Hermitian part. If the Hermitian part prevails in the perturbation $\Delta\mathbf{A}$, we have $D < 0$. In particular, $D = -\operatorname{Im}^2\zeta < 0$ for a purely Hermitian perturbation $\Delta\mathbf{A}$.

Let us assume that the vector $\mathbf{p}$ consists of only two components p_1 and p_2, and consider surfaces (18) and (19) for different kinds of perturbation $\Delta\mathbf{A}(\mathbf{p})$. Consider first the case $D < 0$. Then, the eigensheets $\operatorname{Re}\lambda_+(\mathbf{p})$ and $\operatorname{Re}\lambda_-(\mathbf{p})$ are separate, see figure 2(*a*). Indeed, for $D \leqslant -\operatorname{Re}^2\zeta$ the inequality $\operatorname{Re} c \geqslant 0$ holds for all variations of parameters, see equation (16). In the case when $-\operatorname{Re}^2\zeta < D < 0$ the equation $\operatorname{Re} c = 0$ with expressions (13) defines an ellipse in the plane of parameters (p_1, p_2). Inside the ellipse we have $\operatorname{Re} c < 0$ and outside $\operatorname{Re} c > 0$. The equation $\operatorname{Im} c = 0$ defines a line in parameter plane. The line and the ellipse have no common points for $D < 0$ since there are no real solutions of the equation $c = 0$. Hence, for $D < 0$ conditions (20) are not fulfilled and the real parts of the eigenvalues avoid crossing. As the size of the complex perturbation decreases ($\varepsilon \to 0$), the two sheets come closer and touch each other at the point $(\mathbf{p}_0, \lambda_0)$ for $\varepsilon = 0$ forming the

diabolic singularity. The sheets $\operatorname{Im}\lambda_+(\mathbf{p})$ and $\operatorname{Im}\lambda_-(\mathbf{p})$ of the eigensurface (19) intersect along the line

$$\operatorname{Im} c/2 = (x + \operatorname{Re}\xi)\operatorname{Im}\xi + (y + \operatorname{Re}\eta)\operatorname{Im}\eta - \operatorname{Re}\zeta\operatorname{Im}\zeta = 0, \qquad \operatorname{Im}\lambda_\pm = \operatorname{Im}\mu, \tag{28}$$

given by conditions (21). Note that, by using (22), one can show that the angle of intersection of the imaginary eigensheets is small of order ε and tends to zero as $\varepsilon \to 0$.

In the case $D > 0$, the line $\operatorname{Im} c = 0$ and the ellipse $\operatorname{Re} c = 0$ have common points $\mathbf{p}_a$ and $\mathbf{p}_b$ where the eigenvalues couple. Coordinates of these points found from equations (13) are

$$\mathbf{p}_{a,b} = \mathbf{p}_0 + \left(-\frac{2f_{12}^2 x_{a,b} - \left(f_{11}^2 - f_{22}^2\right) y_{a,b}}{f_{12}^1\left(f_{11}^2 - f_{22}^2\right) - f_{12}^2\left(f_{11}^1 - f_{22}^1\right)}, \frac{2f_{12}^1 x_{a,b} - \left(f_{11}^1 - f_{22}^1\right) y_{a,b}}{f_{12}^1\left(f_{11}^2 - f_{22}^2\right) - f_{12}^2\left(f_{11}^1 - f_{22}^1\right)} \right), \tag{29}$$

where $x_{a,b}$ and $y_{a,b}$ are defined by expressions (24) and (25). Here we have assumed that the vectors $\mathbf{f}_{11} - \mathbf{f}_{22}$ and $\mathbf{f}_{12}$ are linearly independent. Note that the points $\mathbf{p}_a$ and $\mathbf{p}_b$ coincide in the degenerate case $D = 0$.

According to conditions (20) the real eigensheets $\operatorname{Re}\lambda_+(\mathbf{p})$ and $\operatorname{Re}\lambda_-(\mathbf{p})$ are glued in the interval $[\mathbf{p}_a, \mathbf{p}_b]$ of the line

$$\operatorname{Im} c/2 = (x + \operatorname{Re}\xi)\operatorname{Im}\xi + (y + \operatorname{Re}\eta)\operatorname{Im}\eta - \operatorname{Re}\zeta\operatorname{Im}\zeta = 0, \qquad \operatorname{Re}\lambda_\pm = \lambda_0' + \operatorname{Re}\mu. \tag{30}$$

The surface of real eigenvalues (18) is called a 'double coffee filter' (Keck *et al* 2003). The unfolding of a diabolic point into the double coffee filter is shown in figure 2(*b*).

From conditions (21), it follows that the imaginary eigensheets $\operatorname{Im}\lambda_+(\mathbf{p})$ and $\operatorname{Im}\lambda_-(\mathbf{p})$ are connected along the straight line (28) where the interval $[\mathbf{p}_a, \mathbf{p}_b]$ is excluded, see figure 2(*b*). According to formulae (22) the angle of intersection of the imaginary eigensheets tends to π as the points $\mathbf{p}_a$ and $\mathbf{p}_b$ are approached, since $\operatorname{Re} c$ goes to zero. At far distances from the interval $[\mathbf{p}_a, \mathbf{p}_b]$, this angle becomes small of order ε. With the decrease of the size of complex perturbation ε the interval shrinks and the angle of intersection goes to zero. At $\varepsilon = 0$ the imaginary parts of the eigenvalues coincide: $\operatorname{Im}\lambda_+ = \operatorname{Im}\lambda_- = 0$. Note that in crystal optics and acoustics the interval $[\mathbf{p}_a, \mathbf{p}_b]$ is referred to as a 'branch cut', and the points $\mathbf{p}_a, \mathbf{p}_b$ are called 'singular axes', see Shuvalov and Scott (2000), Berry and Dennis (2003) and Ramachandran and Ramaseshan (1961). According to equation (8) the double eigenvalues at $\mathbf{p}_a$ and $\mathbf{p}_b$ possess only one eigenvector and, hence, they are exceptional points (EPs).

Now let us consider the case when the perturbation $\Delta\mathbf{A}(\mathbf{p})$ is real. In this case μ, ξ, η, ζ and hence

$$c = (x + \xi)^2 + (y + \eta)^2 - \zeta^2 \tag{31}$$

are real quantities. According to (12) the eigenvalues $\lambda_\pm$ are complex conjugate if $c < 0$ and real if $c > 0$. The eigenvalues couple for $c = 0$ forming a set consisting of exceptional points with double real eigenvalues.

Consider a system depending on a vector of two parameters $\mathbf{p} = (p_1, p_2)$. Then the equation $c = 0$ with expressions (13) and (31) defines an ellipse in parameter plane; $c < 0$ inside the ellipse and $c > 0$ outside. Real parts of the eigenvalues are given by the equations

$$c \geqslant 0: \quad (\operatorname{Re}\lambda - \lambda_0' - \mu)^2 - (x + \xi)^2 - (y + \eta)^2 = -\zeta^2, \tag{32}$$

$$c \leqslant 0: \quad \operatorname{Re}\lambda = \lambda_0' + \mu. \tag{33}$$

Equation (32) defines a hyperboloid in the space $(p_1, p_2, \operatorname{Re}\lambda)$. Real parts of the eigenvalues $\lambda_\pm$ coincide at the disc determined by equation (33), see figure 3. Imaginary parts of the eigenvalues are

$$c \geqslant 0: \quad \operatorname{Im}\lambda = 0, \tag{34}$$

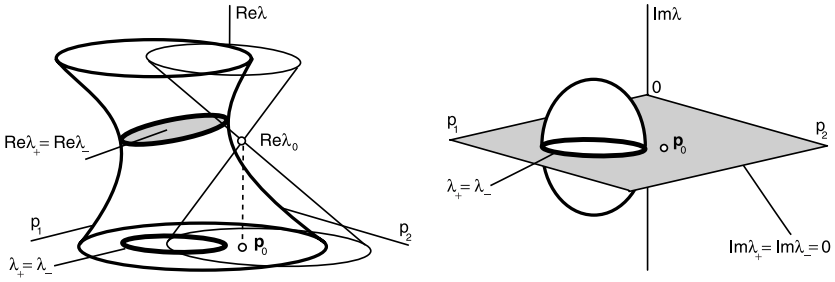

Figure 3. A real non-symmetric perturbation of a diabolic point.

$$c \leqslant 0: \quad \mathrm{Im}^2\,\lambda + (x+\xi)^2 + (y+\eta)^2 = \zeta^2. \tag{35}$$

The imaginary parts are both zero at the points of the plane (34) surrounding the ellipsoid (35) ('a bubble') in the space $(p_1, p_2, \mathrm{Im}\,\lambda)$, see figure 3. The eigenvalues couple at the points of the elliptic ring

$$\lambda_\pm = \lambda_0' + \mu, \qquad (x+\xi)^2 + (y+\eta)^2 = \zeta^2, \tag{36}$$

consisting of exceptional points, see figure 3. For that reason we call it an 'exceptional ring', which is a better name compared with a 'diabolic circle' suggested by Mondragon and Hernandez (1993, 1996).

Note that for the real symmetric perturbation $\Delta\mathbf{A}$, we have $\zeta = 0$ according to equations (7) and (14). Then, the radius of the exceptional ring in equation (36) is zero and the perturbation preserves the diabolic point, only shifting it.

Finally, it is instructive to consider deformations of the surfaces (32), (33) and (34), (35) as the real perturbation becomes complex. If the imaginary part of the perturbation $\mathrm{Im}\,\Delta\mathbf{A}$ is such that $D < 0$, then the parts of the hyperboloid (32) connected by the disc (33) are separated into the two smooth surfaces described by equation (18). On the other hand, the ellipsoid (35) surrounded by the plane (34) is foliated into two sheets crossing each other along the line $\mathrm{Im}\,c = 0$, see figure 2(*a*). Recall that the line $\mathrm{Im}\,c = 0$ does not intersect the ellipse $\mathrm{Re}\,c = 0$. When $D > 0$, the disc (33) foliates into two sheets crossing along the interval $[\mathbf{p}_a, \mathbf{p}_b]$, where the points $\mathbf{p}_a$ and $\mathbf{p}_b$ are given by expression (29). As the size of the imaginary part of the perturbation $\mathrm{Im}\,\Delta\mathbf{A}$ increases, the angle of intersection of real eigensheets grows. In this way, the purely imaginary perturbation deforms the hyperboloid (32) into the double coffee filter (18), see figure 2(*b*). The ellipsoid (35) surrounded by the plane (34) is transformed into two smooth sheets intersecting along the line $\mathrm{Im}\,c = 0$, where the interval $[\mathbf{p}_a, \mathbf{p}_b]$ is excluded. The angle of intersection grows as the size of the perturbation $\mathrm{Im}\,\Delta\mathbf{A}$ increases.

4. Unfolding of a diabolic singularity for Hermitian matrices

Let us consider a multiparameter Hermitian matrix $\mathbf{A}(\mathbf{p})$. Assume that $\mathbf{p}_0$ is a diabolic point, where the matrix $\mathbf{A}_0 = \mathbf{A}(\mathbf{p}_0)$ has a double real eigenvalue λ_0 with two eigenvectors. The splitting of λ_0 into a pair of simple real eigenvalues λ_+ and λ_- is described by expressions (3), (4), where the vectors $\mathbf{f}_{11}$ and $\mathbf{f}_{22}$ are real and the vectors $\mathbf{f}_{12} = \overline{\mathbf{f}}_{21}$ are complex conjugate. By using expression (3), we find

$$\lambda_\pm = \lambda_0' \pm \sqrt{x^2 + y^2 + z^2}, \tag{37}$$

where λ_0', x, y and z are real quantities depending linearly on the perturbation of parameters $\Delta\mathbf{p}$ as follows:

$$\lambda_0' = \lambda_0 + \frac{\langle \mathbf{f}_{11} + \mathbf{f}_{22}, \Delta\mathbf{p}\rangle}{2}, \qquad x = \frac{\langle \mathbf{f}_{11} - \mathbf{f}_{22}, \Delta\mathbf{p}\rangle}{2},$$
$$y = \langle \operatorname{Re}\mathbf{f}_{12}, \Delta\mathbf{p}\rangle, \qquad z = \langle \operatorname{Im}\mathbf{f}_{12}, \Delta\mathbf{p}\rangle. \tag{38}$$

The eigenvalues coincide if $x = y = z = 0$. Thus, if the system depends on three parameters and the real vectors $\mathbf{f}_{11} - \mathbf{f}_{22}$, $\operatorname{Re}\mathbf{f}_{12}$ and $\operatorname{Im}\mathbf{f}_{12}$ are linearly independent, the eigenvalues λ_+ and λ_- split for any nonzero perturbation $\Delta\mathbf{p}$. For more than three parameters, the equations $x = y = z = 0$ with relations (38) provide a plane of diabolic points in parameter space. This plane has dimension $n - 3$, which agrees with the well-known fact that the diabolic point is a codimension 3 phenomenon for Hermitian systems (Von Neumann and Wigner 1929, Arnold 1972).

Now let us consider a general non-Hermitian perturbation of the system $\mathbf{A}(\mathbf{p}) + \Delta\mathbf{A}(\mathbf{p})$, assuming that the size of perturbation at the diabolic point $\varepsilon = \|\Delta\mathbf{A}(\mathbf{p}_0)\|$ is small. The two eigenvalues λ_+ and λ_-, which become complex due to non-Hermitian perturbation, are given by asymptotic expressions (6), (7). With the use of the new coordinates (38), we write expression (6) as

$$\lambda_\pm = \lambda_0' + \mu \pm \sqrt{c}, \tag{39}$$

where

$$c = (x + \xi)^2 + (y + \eta)^2 + (z - \mathrm{i}\zeta)^2, \tag{40}$$

and μ, ξ, η, ζ are small complex quantities of order ε given by expressions (14).

The eigenvalues couple ($\lambda_+ = \lambda_-$) if $c = 0$. This yields two equations

$$\operatorname{Re} c = (x + \operatorname{Re}\xi)^2 + (y + \operatorname{Re}\eta)^2 + (z + \operatorname{Im}\zeta)^2 - (\operatorname{Im}^2\xi + \operatorname{Im}^2\eta + \operatorname{Re}^2\zeta) = 0, \tag{41}$$

$$\operatorname{Im} c = 2(\operatorname{Im}\xi(x + \operatorname{Re}\xi) + \operatorname{Im}\eta(y + \operatorname{Re}\eta) - \operatorname{Re}\zeta(z + \operatorname{Im}\zeta)) = 0. \tag{42}$$

Equation (41) defines a sphere in (x, y, z) space with the centre at $(-\operatorname{Re}\xi, -\operatorname{Re}\eta, -\operatorname{Im}\zeta)$ and the radius $\sqrt{\operatorname{Im}^2\xi + \operatorname{Im}^2\eta + \operatorname{Re}^2\zeta}$, which are small of order ε. Equation (42) yields a plane passing through the centre of the sphere. The sphere and the plane intersect along a circle. Points of this circle determine values of parameters, for which the eigenvalues $\lambda_\pm$ coincide. Since $c = 0$ at the coupling point, expression (8) for the eigenvectors takes the form

$$\mathbf{u}_\pm = \alpha_\pm^\varepsilon \mathbf{u}_1 + \beta_\pm^\varepsilon \mathbf{u}_2, \qquad \frac{\alpha_\pm^\varepsilon}{\beta_\pm^\varepsilon} = \frac{y + \mathrm{i}z + \eta + \zeta}{-x - \xi} = \frac{x + \xi}{y - \mathrm{i}z + \eta - \zeta}. \tag{43}$$

Thus, all points of the circle are exceptional points, where the two eigenvectors $\mathbf{u}_-$ and $\mathbf{u}_+$ merge in addition to the coupling of the eigenvalues λ_+ and λ_-. By using linear expressions (38), the set of exceptional points is found in the original parameter space $\mathbf{p}$. The exceptional circle in (x, y, z) space is transformed into an exceptional elliptic ring in three-parameter space $\mathbf{p}$, see figure 4.

Let us consider the plane (42), at which the quantity c is real. By formula (39), the real parts of the eigenvalues $\lambda_\pm$ coincide inside the exceptional ring, where $c < 0$, and the imaginary parts of $\lambda_\pm$ coincide outside the exceptional ring, where $c > 0$, see the dark and light shaded areas in figure 4.

We see that, under a general complex perturbation, a diabolic point of a three-parameter Hermitian system bifurcates into an exceptional ring. This ring has elliptic shape and grows proportionally to the size of perturbation ε. The real and imaginary parts of the eigenvalues $\lambda_\pm$ coincide, respectively, inside and outside the exceptional ring in the plane of the ring.

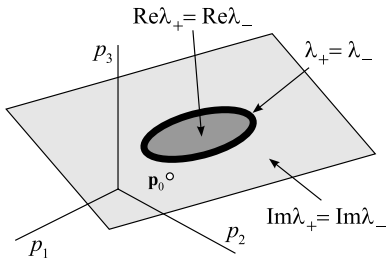

Figure 4. Unfolding of a diabolic point into an exceptional ring in parameter space.

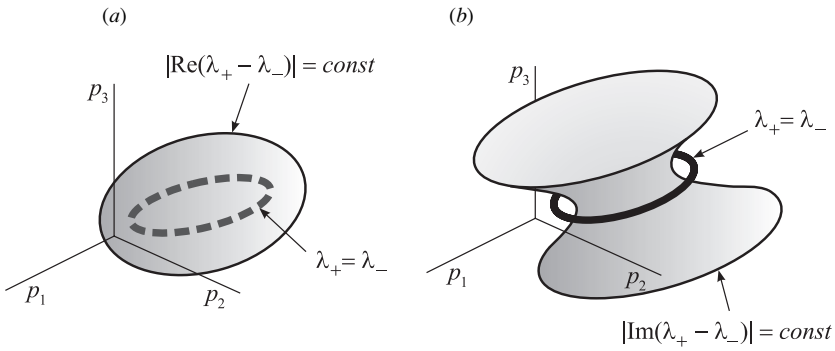

Figure 5. Surfaces corresponding to coincident real or imaginary parts of eigenvalues.

Note that for the Hermitian perturbation $\Delta\mathbf{A}$, one has $\operatorname{Im}\xi = \operatorname{Im}\eta = \operatorname{Re}\zeta = 0$ as follows from equations (7) and (14). Hence, the radius of the exceptional ring is zero, which means that the Hermitian perturbation just shifts the diabolic point without splitting it.

Finally, let us study the stratification of parameter space given by the condition $|\operatorname{Re}(\lambda_+ - \lambda_-)| = \text{const}$. For problems of quantum mechanics, this difference describes the size of a gap between two adjacent energy levels. By using expression (39), we find $(\lambda_+ - \lambda_-)^2 = 4c$. Separating real and imaginary parts in this equation and extracting $\operatorname{Im}(\lambda_+ - \lambda_-)$, we get

$$\operatorname{Re}^4(\lambda_+ - \lambda_-) - 4\operatorname{Re}^2(\lambda_+ - \lambda_-)\operatorname{Re} c - 4\operatorname{Im}^2 c = 0, \tag{44}$$

where $\operatorname{Re} c$ and $\operatorname{Im} c$ are given by the first equalities in (41) and (42). Given a fixed value of $|\operatorname{Re}(\lambda_+ - \lambda_-)|$, equation (44) with (41), (42) and (38) defines an ellipsoid in three-parameter space enclosing the exceptional ring, see figure 5(*a*). A similar analysis provides the equation

$$\operatorname{Im}^4(\lambda_+ - \lambda_-) + 4\operatorname{Im}^2(\lambda_+ - \lambda_-)\operatorname{Re} c - 4\operatorname{Im}^2 c = 0 \tag{45}$$

for a surface given by the condition $|\operatorname{Im}(\lambda_+ - \lambda_-)| = \text{const}$. In three-parameter space equation (45) defines a hyperboloid surrounded by the exceptional ring, see figure 5(*b*).

5. Unfolding of optical singularities of birefringent crystals

Optical properties of a non-magnetic dichroic chiral anisotropic crystal are characterized by the inverse dielectric tensor $\boldsymbol{\eta}$, which relates the vectors of electric field $\mathbf{E}$ and the displacement $\mathbf{D}$ as (Landau *et al* 1984)

$$\mathbf{E} = \boldsymbol{\eta}\mathbf{D}. \tag{46}$$

A monochromatic plane wave of frequency ω that propagates in a direction specified by a real unit vector $\mathbf{s} = (s_1, s_2, s_3)$ has the form

$$\mathbf{D}(\mathbf{r}, t) = \mathbf{D}(\mathbf{s}) \exp \mathrm{i}\omega\left(\frac{n(\mathbf{s})}{c}\mathbf{s}^T\mathbf{r} - t\right), \tag{47}$$

where $n(\mathbf{s})$ is a refractive index, and $\mathbf{r}$ is the real vector of spatial coordinates. With the wave (47) and the constitutive relation (46) Maxwell's equations after some elementary manipulations yield (see, e.g., Berry and Dennis (2003))

$$\boldsymbol{\eta}\mathbf{D}(\mathbf{s}) - \mathbf{s}\mathbf{s}^T\boldsymbol{\eta}\mathbf{D}(\mathbf{s}) = \frac{1}{n^2(\mathbf{s})}\mathbf{D}(\mathbf{s}). \tag{48}$$

Multiplying equation (48) by the vector $\mathbf{s}^T$ from the left, we find that for plane waves the vector $\mathbf{D}$ is always orthogonal to the direction $\mathbf{s}$, i.e., $\mathbf{s}^T\mathbf{D}(\mathbf{s}) = 0$. By using this condition, we write (48) in the form of the eigenvalue problem

$$\left[(\mathbf{I} - \mathbf{s}\mathbf{s}^T)\boldsymbol{\eta}(\mathbf{I} - \mathbf{s}\mathbf{s}^T)\right]\mathbf{u} = \lambda\mathbf{u}, \tag{49}$$

where $\lambda = n^{-2}$, $\mathbf{u} = \mathbf{D}$ and $\mathbf{I}$ is the identity matrix. Since $\mathbf{I} - \mathbf{s}\mathbf{s}^T$ is a singular matrix, one of the eigenvalues is always zero. Let us denote the other two eigenvalues by λ_+ and λ_-. These eigenvalues determine refractive indices n, and the corresponding eigenvectors yield polarizations.

The inverse dielectric tensor is described by a complex non-Hermitian matrix $\boldsymbol{\eta} = \boldsymbol{\eta}_{\mathrm{transp}} + \boldsymbol{\eta}_{\mathrm{dichroic}} + \boldsymbol{\eta}_{\mathrm{chiral}}$. The symmetric part of $\boldsymbol{\eta}$ consisting of the real matrix $\boldsymbol{\eta}_{\mathrm{transp}}$ and imaginary matrix $\boldsymbol{\eta}_{\mathrm{dichroic}}$ constitute the anisotropy tensor, which describes the birefringence of the crystal. For a transparent crystal, the anisotropy tensor is real and is represented only by the matrix $\boldsymbol{\eta}_{\mathrm{transp}}$; for a crystal with linear dichroism it is complex. Choosing coordinate axes along the principal axes of $\boldsymbol{\eta}_{\mathrm{transp}}$, we have

$$\boldsymbol{\eta}_{\mathrm{transp}} = \begin{pmatrix} \eta_1 & 0 & 0 \\ 0 & \eta_2 & 0 \\ 0 & 0 & \eta_3 \end{pmatrix}. \tag{50}$$

The matrix

$$\boldsymbol{\eta}_{\mathrm{dichroic}} = \mathrm{i}\begin{pmatrix} \eta^d_{11} & \eta^d_{12} & \eta^d_{13} \\ \eta^d_{12} & \eta^d_{22} & \eta^d_{23} \\ \eta^d_{13} & \eta^d_{23} & \eta^d_{33} \end{pmatrix} \tag{51}$$

describes linear dichroism (absorption). The matrix $\boldsymbol{\eta}_{\mathrm{chiral}}$ gives the antisymmetric part of $\boldsymbol{\eta}$ describing chirality (optical activity) of the crystal. It is determined by the optical activity vector $\mathbf{g} = (g_1, g_2, g_3)$ depending linearly on $\mathbf{s}$ as

$$\boldsymbol{\eta}_{\mathrm{chiral}} = \mathrm{i}\begin{pmatrix} 0 & -g_3 & g_2 \\ g_3 & 0 & -g_1 \\ -g_2 & g_1 & 0 \end{pmatrix}, \qquad \mathbf{g} = \boldsymbol{\gamma}\mathbf{s} = \begin{pmatrix} \gamma_{11} & \gamma_{12} & \gamma_{13} \\ \gamma_{12} & \gamma_{22} & \gamma_{23} \\ \gamma_{13} & \gamma_{23} & \gamma_{33} \end{pmatrix}\begin{pmatrix} s_1 \\ s_2 \\ s_3 \end{pmatrix}, \tag{52}$$

where $\boldsymbol{\gamma}$ is a symmetric optical activity tensor; this tensor has an imaginary part for a material with circular dichroism.

In the present formulation Berry and Dennis (2003) studied the problem of determining the surfaces of the refractive indices as functions of the components of direction vector $\mathbf{s}$. In their paper the reduction to two dimensions was carried out. Our intention here is to consider the original three-dimensional problem with the inverse dielectric tensor taken in its most general form. Unlike Berry and Dennis (2003) we would like to study the unfolding of the eigenvalue surfaces near the diabolic point in terms of the original problem parameters.

First, consider a transparent non-chiral crystal, when $\boldsymbol{\eta}_{\text{dichroic}} = 0$ and $\boldsymbol{\gamma} = 0$. Then the matrix

$$\mathbf{A}(\mathbf{p}) = (\mathbf{I} - \mathbf{s}\mathbf{s}^T)\boldsymbol{\eta}_{\text{transp}}(\mathbf{I} - \mathbf{s}\mathbf{s}^T) \tag{53}$$

is real symmetric and depends on a vector of two parameters $\mathbf{p} = (s_1, s_2)$ (see Berry and Dennis (2003) for other ways of introducing two parameters). The third component of the direction vector $\mathbf{s}$ is found as $s_3 = \pm\sqrt{1 - s_1^2 - s_2^2}$, where the cases of two different signs should be considered separately. Below we assume that three dielectric constants $\eta_1 > \eta_2 > \eta_3$ are different. This corresponds to biaxial anisotropic crystals.

The nonzero eigenvalues $\lambda_\pm$ of the matrix $\mathbf{A}(\mathbf{p})$ are found explicitly in the form (Lewin 1994)

$$\lambda_\pm = \frac{\operatorname{trace}\mathbf{A}}{2} \pm \frac{1}{2}\sqrt{2\operatorname{trace}(\mathbf{A}^2) - (\operatorname{trace}\mathbf{A})^2}. \tag{54}$$

The eigenvalues $\lambda_\pm$ are the same for opposite directions $\mathbf{s}$ and $-\mathbf{s}$. By using (50) and (53) in (54), it is straightforward to show that two eigenvalues λ_+ and λ_- couple at

$$\begin{aligned} &\mathbf{s}_0 = (S_1, S_2, S_3), \qquad \lambda_0 = \eta_2; \qquad S_1 = \pm\sqrt{(\eta_1 - \eta_2)/(\eta_1 - \eta_3)}, \\ &S_2 = 0, \qquad S_3 = \pm\sqrt{1 - S_1^2}, \end{aligned} \tag{55}$$

which determine four diabolic points (for two signs of S_1 and S_3), also called optic axes (Ramachandran and Ramaseshan 1961). The double eigenvalue $\lambda_0 = \eta_2$ of the matrix $\mathbf{A}_0 = \mathbf{A}(\mathbf{p}_0)$, $\mathbf{p}_0 = (S_1, 0)$ possesses two eigenvectors

$$\mathbf{u}_1 = \begin{pmatrix} 0 \\ 1 \\ 0 \end{pmatrix}, \qquad \mathbf{u}_2 = \begin{pmatrix} S_3 \\ 0 \\ -S_1 \end{pmatrix}, \tag{56}$$

satisfying normalization conditions (2). Using expressions (53) and (56), we evaluate the vectors $\mathbf{f}_{ij}$ with components (4) for optic axes (55) as

$$\mathbf{f}_{11} = (0, 0), \qquad \mathbf{f}_{22} = (2(\eta_3 - \eta_1)S_1, 0), \qquad \mathbf{f}_{12} = \mathbf{f}_{21} = (0, (\eta_3 - \eta_1)S_1S_3). \tag{57}$$

By using (55) and (57) in (10), we obtain the local asymptotic expression for the cone singularities in the space (s_1, s_2, λ) as

$$(\lambda - \eta_2 - (\eta_3 - \eta_1)S_1(s_1 - S_1))^2 = (\eta_3 - \eta_1)^2 S_1^2\big((s_1 - S_1)^2 + S_3^2 s_2^2\big). \tag{58}$$

Equation (58) is valid for each of the four optic axes (55).

As an example, consider the case of $\eta_1 = 0.5$, $\eta_2 = 0.4$, $\eta_3 = 0.1$. Conical surfaces (58) are shown in figure 6 together with the exact eigenvalue surfaces (54). The two optic axes presented in figure 6 are $\mathbf{s}_0 = (\pm 1/2, 0, \sqrt{3}/2)$ with the double eigenvalue $\lambda_0 = 2/5$; the eigenvalue surfaces for the opposite directions $\mathbf{s}_0 = (\pm 1/2, 0, -\sqrt{3}/2)$ are exactly the same.

Now let us assume that the crystal possesses absorption and chirality. Then the matrix family (53) takes a complex perturbation $\mathbf{A}(\mathbf{p}) + \Delta\mathbf{A}(\mathbf{p})$, where

$$\Delta\mathbf{A}(\mathbf{p}) = (\mathbf{I} - \mathbf{s}\mathbf{s}^T)(\boldsymbol{\eta}_{\text{dichroic}} + \boldsymbol{\eta}_{\text{chiral}})(\mathbf{I} - \mathbf{s}\mathbf{s}^T). \tag{59}$$

Assume that the absorption and chirality are weak, i.e., $\varepsilon = \|\boldsymbol{\eta}_{\text{dichroic}}\| + \|\boldsymbol{\eta}_{\text{chiral}}\|$ is small. Then we can use the asymptotic formulae of sections 2 and 3 to describe unfolding of diabolic singularities of the eigenvalue surfaces. For this purpose, we need to know only the value of the perturbation $\Delta\mathbf{A}$ at the optic axes of the transparent non-chiral crystal $\mathbf{s}_0$.

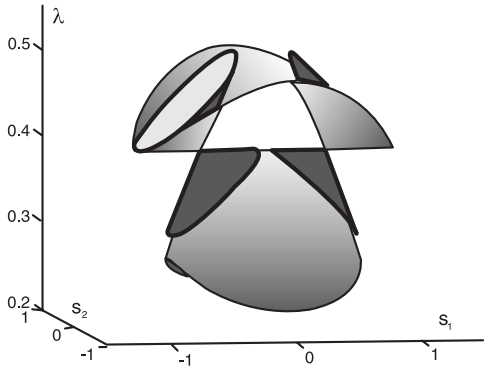

Figure 6. Diabolic singularities near optic axes and their local approximations.

Substituting matrix (59) evaluated at optic axes (55) into expression (7), we obtain

$$\begin{aligned}
&\varepsilon_{11} = \mathrm{i}\eta^d_{22}, \qquad \varepsilon_{22} = \mathrm{i}\eta^d_{11}S_3^2 - 2\mathrm{i}\eta^d_{13}S_1S_3 + \mathrm{i}\eta^d_{33}S_1^2,\\
&\varepsilon_{12} = -\mathrm{i}\big(\eta^d_{23} + \gamma_{11}S_1 + \gamma_{13}S_3\big)S_1 + \mathrm{i}\big(\eta^d_{12} - \gamma_{13}S_1 - \gamma_{33}S_3\big)S_3,\\
&\varepsilon_{21} = -\mathrm{i}\big(\eta^d_{23} - \gamma_{11}S_1 - \gamma_{13}S_3\big)S_1 + \mathrm{i}\big(\eta^d_{12} + \gamma_{13}S_1 + \gamma_{33}S_3\big)S_3.
\end{aligned} \tag{60}$$

By using formulae (14), we get

$$\begin{aligned}
&\mu = \mathrm{i}\big(\eta^d_{22} + \eta^d_{11}S_3^2 - 2\eta^d_{13}S_1S_3 + \eta^d_{33}S_1^2\big)/2,\\
&\xi = \mathrm{i}\big(\eta^d_{22} - \eta^d_{11}S_3^2 + 2\eta^d_{13}S_1S_3 - \eta^d_{33}S_1^2\big)/2,\\
&\eta = \mathrm{i}\big(\eta^d_{12}S_3 - \eta^d_{23}S_1\big),\\
&\zeta = -\mathrm{i}\big(\gamma_{11}S_1^2 + 2\gamma_{13}S_1S_3 + \gamma_{33}S_3^2\big).
\end{aligned} \tag{61}$$

We see that μ, ξ and η are purely imaginary numbers depending only on dichroic properties of the crystal (absorption). The quantity ζ depends only on chiral properties of the crystal; ζ is purely imaginary if the optical activity tensor $\boldsymbol{\gamma}$ is real.

Singularities for crystals with weak dichroism and chirality were studied recently in Berry and Dennis (2003). It was shown that the double coffee filter singularity arises in absorption-dominated crystals, and the sheets of real parts of eigenvalues are separated in chirality-dominated crystals. According to the results of section 3, these two cases are explicitly determined by the conditions $D > 0$ and $D < 0$, respectively, where $D = \mathrm{Im}^2\,\xi + \mathrm{Im}^2\,\eta - \mathrm{Im}^2\,\zeta$. These conditions are new and important because they provide quantitative definitions of absorption-dominated and chirality-dominated regimes for unfolding of the diabolic singularity in terms of components of the inverse dielectric tensor. Indeed, according to (61), ξ and η depend linearly on all the components of the tensor $\boldsymbol{\eta}_{\mathrm{dichroic}}$, while ζ depends linearly on the components γ_{ij}, $i, j = 1, 3$, of the optical activity tensor $\boldsymbol{\gamma}$.

Note that according to the sign of the quantity D taken at different optic axes, we can classify crystals by their optic properties. For example, the important case is a chirality-dominated crystal with $D < 0$ for all four optic axes. Then real parts of the eigenvalues separate for all directions $\mathbf{s}$.

There are four optic axes (55), which determine two pairs of opposite space direction $\pm\mathbf{s}_0$. It is easy to see that the unfolding conditions coincide for the optic axes given by opposite directions, while these conditions are different for different pairs of optic axes. In

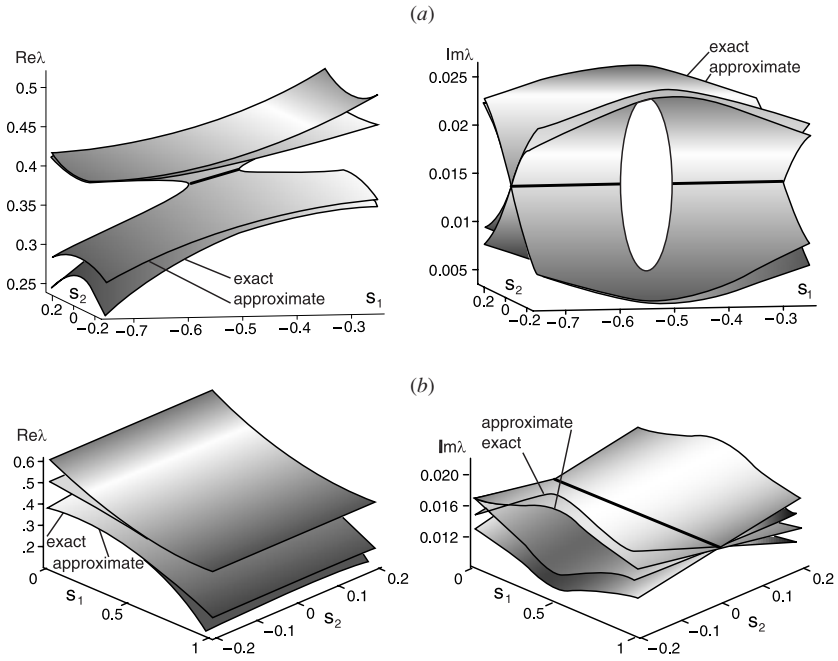

Figure 7. Unfolding of singularities near optic axes.

the absorption-dominated case, when diabolic singularities unfold into coffee filters near two opposite optic axes $\pm\mathbf{s}_0 = \pm(S_1, 0, S_3)$, the four exceptional points of eigenvalue coupling $\pm\mathbf{s}_a$ and $\pm\mathbf{s}_b$ (also called singular axes) appear. By using (57) in (13), we obtain the asymptotic formulae

$$s_1^{a,b} = S_1 + \frac{x_{a,b}}{(\eta_1 - \eta_3)S_1}, \qquad s_2^{a,b} = \frac{y_{a,b}}{(\eta_3 - \eta_1)S_1 S_3}, \qquad s_3^{a,b} = \sqrt{1 - \left(s_1^{a,b}\right)^2 - \left(s_2^{a,b}\right)^2}, \quad (62)$$

for the components of the vectors $\mathbf{s}_{a,b}$, where $x_{a,b}$ and $y_{a,b}$ are found by using expressions (24), (25) and (61). In particular, for non-chiral crystals, we have $\zeta = 0$. Then expressions (24), (25) yield $x_{a,b} = \pm\mathrm{Im}\,\eta = \pm\left(\eta_{12}^d S_3 - \eta_{23}^d S_1\right)$ and $y_{a,b} = \mp\mathrm{Im}\,\xi = \pm\left(\eta_{22}^d - \eta_{11}^d S_3^2 + 2\eta_{13}^d S_1 S_3 - \eta_{33}^d S_1^2\right)/2$.

The equation $\mathrm{Im}\,c = 0$ determines a line of singularities in the parameter space $\mathbf{p} = (s_1, s_2)$. By using (57), (61) in (13), (17), we find this line in the form

$$(s_1 - S_1)S_1(\eta_1 - \eta_3)\mathrm{Im}\,\xi - s_2 S_1 S_3(\eta_1 - \eta_3)\mathrm{Im}\,\eta - \mathrm{Re}\,\zeta\,\mathrm{Im}\,\zeta = 0. \quad (63)$$

In the absorption-dominated case, line (63) contains two exceptional points $\mathbf{p}_{a,b} = \left(s_1^{a,b}, s_2^{a,b}\right)$ corresponding to the singular axes $\mathbf{s}_{a,b}$. A segment between the points $\mathbf{p}_a$ and $\mathbf{p}_b$ corresponds to the coincidence of real parts of the eigenvalues $\mathrm{Re}\,\lambda_+ = \mathrm{Re}\,\lambda_-$, while imaginary parts of the eigenvalues $\mathrm{Im}\,\lambda_+ = \mathrm{Im}\,\lambda_-$ merge at points of line (63) outside this segment, see figure 2(*b*). In the chirality-dominated case, when singular axes do not appear, imaginary parts of the eigenvalues $\mathrm{Im}\,\lambda_+ = \mathrm{Im}\,\lambda_-$ coincide at points of the whole line (63), see figure 2(*a*). If the optical activity tensor $\boldsymbol{\gamma}$ is real or purely imaginary, then the line of singularities (63) passes through the diabolic point $\mathbf{p}_0$, and the position of this line does not depend on $\boldsymbol{\gamma}$.

As a numerical example, let us consider a crystal possessing weak absorption and chirality described by tensors (51), (52) with

$$\boldsymbol{\eta}_{\text{dichroic}} = \frac{\mathrm{i}}{200}\begin{pmatrix} 3 & 2 & 0 \\ 2 & 3 & 1 \\ 0 & 1 & 3 \end{pmatrix}, \qquad \boldsymbol{\gamma} = \frac{1}{200}\begin{pmatrix} 3 & 1 & 2 \\ 1 & 3 & 1 \\ 2 & 1 & 3 \end{pmatrix}. \tag{64}$$

A corresponding transparent non-chiral crystal is characterized by $\eta_1 = 0.5$, $\eta_2 = 0.4$, $\eta_3 = 0.1$, and its eigenvalue surfaces with two optic axes are presented in figure 6. By using (64) in (61), we find that the condition $D = \frac{7}{160\,000}(4\sqrt{3} - 5) > 0$ is satisfied for the left optic axis $\mathbf{s}_0 = (-1/2, 0, \sqrt{3}/2)$. Hence, the diabolic singularity bifurcates into a double coffee filter with two exceptional points whose coordinates according to expressions (62) are

$$\mathbf{p}_a = \left(-\frac{1}{2} - \frac{1}{80}\sqrt{-35 + 28\sqrt{3}}, 0\right), \qquad \mathbf{p}_b = \left(-\frac{1}{2} + \frac{1}{80}\sqrt{-35 + 28\sqrt{3}}, 0\right). \tag{65}$$

Local approximations of the eigenvalue surfaces are given by expressions (18), (19), where

$$\operatorname{Re} c = \frac{35 - 28\sqrt{3}}{160\,000} + \frac{1}{25}(s_1 + 1/2)^2 + \frac{3}{100}s_2^2, \qquad \operatorname{Im} c = -\frac{6 + \sqrt{3}}{2000}s_2. \tag{66}$$

Figure 7(*a*) shows these local approximations compared with the exact eigenvalue surfaces given by (54). For the right optic axis $\mathbf{s}_0 = (1/2, 0, \sqrt{3}/2)$, the condition $D = -\frac{7}{160\,000}(4\sqrt{3} + 5) < 0$ is satisfied. Hence, the eigenvalue sheets (for real parts) separate under the bifurcation of the right diabolic singularity. Approximate and exact eigenvalue surfaces are shown in figure 7(*b*). The approximations are given by expressions (18), (19), where

$$\operatorname{Re} c = \frac{35 + 28\sqrt{3}}{160\,000} + \frac{1}{25}(s_1 - 1/2)^2 + \frac{3}{100}s_2^2, \qquad \operatorname{Im} c = -\frac{6 - \sqrt{3}}{2000}s_2. \tag{67}$$

We observe that the unfolding types are different for different optic axes. As is seen from figure 7, the asymptotic formulae provide an accurate description for unfolding of eigenvalue surfaces near diabolic points.

6. Conclusion

Non-Hermitian Hamiltonians and matrices usually appear in physics when dissipative and other non-conservative effects are taken into account. The known examples are complex refractive indices in optics and complex potentials describing the scattering of electrons or x-rays. Traditionally, non-Hermitian matrices appear in physics as a perturbation of Hermitian matrices. As stated in Berry (2004), Hermitian physics differs radically from non-Hermitian physics in the case of coalescence (coupling) of eigenvalues. In the present paper we have studied this important case carefully. We gave an analytical description for unfolding of eigenvalue surfaces due to an arbitrary complex perturbation with the singularities known in the literature as a 'double coffee filter' and a 'diabolic circle'. As an application of the presented theory, we found explicit asymptotic expressions for the surfaces of refractive indices in crystal optics in a rather general formulation and obtained a simple condition for the origination of a branch cut in the absorption-dominated crystals in terms of the components of anisotropy and optical activity tensors. We emphasize that the developed theory requires only eigenvectors and derivatives of the matrices taken at the singular point, while the size of the matrix and its dependence on parameters are arbitrary. This makes the presented theory powerful and practical for a wide class of physical problems. The given physical example from crystal optics demonstrates the applicability and accuracy of the theory.

Acknowledgments

The work is supported by the research grants RFBR 03-01-00161, CRDF-BRHE Y1-MP-06-19 and CRDF-BRHE Y1-M-06-03.

References

Arnold V I 1972 Modes and quasimodes *Funkt. Anal. Pril.* **6** 12–20 (in Russian)

Berry M V 2004 Physics of non-Hermitian degeneracies *Czech. J. Phys.* **54** 1039–47

Berry M V and Dennis M R 2003 The optical singularities of birefringent dichroic chiral crystals *Proc. R. Soc. Lond.* A **459** 1261–92

Berry M V and Wilkinson M 1984 Diabolical points in the spectra of triangles *Proc. R. Soc. Lond.* A **392** 15–43

Dembowsky C, Dietz B, Gräf H D, Harney H L, Heine A, Heiss W D and Richter A 2003 Observation of a chiral state in a microwave cavity *Phys. Rev. Lett.* **90** 034101

Dembowsky C, Gräf H D, Harney H L, Heine A, Heiss W D, Rehfeld H and Richter A 2001 Experimental observation of the topological structure of exceptional points *Phys. Rev. Lett.* **86** 787–90

Heiss W D 2004 Exceptional points of non-Hermitian operators *J. Phys. A: Math. Gen.* **37** 2455–64

Keck F, Korsch H J and Mossmann S 2003 Unfolding a diabolic point: a generalized crossing scenario *J. Phys. A: Math. Gen.* **36** 2125–37

Korsch H J and Mossmann S 2003 Stark resonances for a double δ quantum well: crossing scenarios, exceptional points and geometric phases *J. Phys. A: Math. Gen.* **36** 2139–53

Landau L D, Lifshitz E M and Pitaevskii L P 1984 *Electrodynamics of Continuous Media* (Oxford: Pergamon)

Lewin M 1994 On the coefficients of the characteristic polynomial of a matrix *Discrete Math.* **125** 255–62

Mondragon A and Hernandez E 1993 Degeneracy and crossing of resonance energy surfaces *J. Phys. A: Math. Gen.* **26** 5595–611

Mondragon A and Hernandez E 1996 Berry phase of a resonant state *J. Phys. A: Math. Gen.* **29** 2567-85

Ramachandran G N and Ramaseshan S 1961 *Crystal Optics* In *Handbuch der Physik* vol XXV/I ed H Flügge (Berlin: Springer)

Seyranian A P, Kirillov O N and Mailybaev A A 2005 Coupling of eigenvalues of complex matrices at diabolic and exceptional points *J. Phys. A: Math. Gen.* **38** 1723–40

Shuvalov A L and Scott N H 2000 On singular features of acoustic wave propagation in weakly anisotropic thermoviscoelasticity *Acta Mech.* **140** 1–15

Stehmann T, Heiss W D and Scholtz F G 2004 Observation of exceptional points in electronic circuits *J. Phys. A: Math. Gen.* **37** 7813–9

Teller E 1937 The crossing of potential surfaces *J. Phys. Chem.* **41** 109–16

Von Neumann J and Wigner E P 1929 Über das Verhalten von Eigenwerten bei adiabatischen Prozessen *Z. Phys.* **30** 467–70